

Arm Movements Evoked by Electrical Stimulation in the Motor Cortex of Monkeys

Michael S. A. Graziano, Tyson N. S. Aflalo, and Dylan F. Cooke

Department of Psychology, Princeton University, Princeton, New Jersey

Submitted 17 December 2004; accepted in final form 22 August 2005

Graziano, Michael S. A., Tyson N. S. Aflalo, and Dylan F. Cooke. Arm movements evoked by electrical stimulation in the motor cortex of monkeys. *J Neurophysiol* 94: 4209–4223, 2005. First published August 25, 2005; doi:10.1152/jn.01303.2004. Electrical stimulation of the motor cortex in monkeys can evoke complex, multi-joint movements including movements of the arm and hand. In this study, we examined these movements in detail and tested whether they showed adaptability to differing circumstances such as to a weight added to the hand. Electrical microstimulation was applied to motor cortex using pulse trains of 500-ms duration (matching the approximate duration of a reach). Arm movement was measured using a high-resolution three-dimensional tracking system. Movement latencies averaged 80.2 ms. Speed profiles were typically smooth and bell-shaped, and the peak speed covaried with movement distance. Stimulation generally evoked a specific final hand position. The convergence of the hand from disparate starting positions to a narrow range of final positions was statistically significant for every site tested (91/91). When a weight was fixed to the hand, for some stimulation sites (74%), the evoked movement appeared to compensate for the weight in that the hand was lifted to a similar final location. For other stimulation sites (26%), the weight caused a significant reduction in final hand height. For about one-half of the sites (54%), the variation in movement of each joint appeared to compensate for the variation in the other joints in a manner that stabilized the hand in a restricted region of space. These findings suggest that at least some of the stimulation-evoked movements reflect relatively high-level, adaptable motor plans.

INTRODUCTION

It has long been debated whether the primate motor cortex controls movement at a level of muscles and joints or at a higher level of coordinated actions. Single neuron recording studies have provided evidence for both low level and high level encoding. Neuronal activity can be correlated with muscle activity, joint rotation, direction of reach, direction of wrist rotation, and speed of the hand (e.g., Georgopoulos et al. 1986; Holdefer and Miller 2002; Kakei et al. 1999; Reina et al. 2001; Scott and Kalaska 1997). Neuronal activity in motor cortex can even be correlated with learned sequences of movements (Lu and Ashe 2005). These studies suggest that motor cortex is heterogeneous and probably encodes a variety of movement parameters, perhaps reflecting the range of movements that the animal typically makes.

Recently we found that electrical microstimulation in the motor cortex of monkeys, when stimulation is applied on a time scale of one-half a second, can result in complex, multi-joint movements (Cooke and Graziano 2004a; Graziano et al.

2002a,b, 2003). These results also support the view that motor cortex controls movement at a relatively complex level. However, the details and level of complexity of these stimulation-evoked movements have not been examined previously. For example, in normal voluntary movement, the hand follows a smooth trajectory with a bell-shaped velocity profile (e.g., Bizzi and Mussa-Ivaldi 1989; Flash and Hogan 1985). If a weight is fixed to the arm, the movement can show compensation, adapting flexibly to the added weight. If one joint deviates from the desired angle, other joints in the arm can compensate, thus bringing the hand closer to the goal position. Do the stimulation evoked movements show similar complexities, or do they instead resemble uncoordinated muscle output?

Three general issues

DETAILS OF MOVEMENT TRAJECTORIES. We measured the stimulation-evoked arm movements in greater detail than had been done previously, using a high-resolution three-dimensional (3-D) tracking system to monitor the position of the hand and the angles of individual arm joints.

COMPENSATION. We fixed a weight to the wrist and tested whether stimulation drove the hand to the same final height, overcoming the weight, or if the added downward force caused the hand to reach a lower final height. We also examined whether the stimulation tended to bring the hand to a similar final location despite trial-by-trial variability in joint angles. If one joint varied from the optimal posture, would the other joints vary in a compensatory fashion to stabilize the hand at a specific location?

CORTICAL LOCALIZATION OF MOVEMENT TYPES. We examined the clustering of movement types on the cortical surface. In our previous publications (Cooke and Graziano 2004a,b; Graziano et al. 2002a), we found a clustering of three types of movement: hand-to-mouth movements; movements resembling defensive or protective gestures; and movements resembling manipulation of objects in central space. The mapping data in the present experiment adds to this emerging picture of the clustering of different types of stimulation-evoked movements.

METHODS

All husbandry, surgical, and behavioral procedures were approved by the Princeton University Institutional Animal Care and Use Committee and the attendant veterinarian and were in accordance with

Address for reprint requests and other correspondence: M. Graziano, Dept. of Psychology, Green Hall, Princeton Univ., Princeton NJ 08544 (E-mail: Graziano@princeton.edu).

The costs of publication of this article were defrayed in part by the payment of page charges. The article must therefore be hereby marked "advertisement" in accordance with 18 U.S.C. Section 1734 solely to indicate this fact.

NIH and USDA guidelines. We studied two adult male *Macaca fascicularis* (4.5 and 7.0 kg).

Surgery

For each monkey, an initial surgical operation was performed under isoflurane anesthesia and strict aseptic conditions, during which an acrylic skullcap was fixed to the skull with bone screws. A steel bolt for holding the head and a 2.5-cm-diam steel chamber for neuronal recording and electrical stimulation were also imbedded in the acrylic. The recording chamber was positioned for a vertical (dorsal-ventral) approach to the precentral gyrus. Each animal recovered from the surgery within 1 wk but was given 2 additional wk to allow the skull to grow tightly around the skull screws. In a subsequent procedure, also under deep anesthesia and aseptic conditions, the recording chamber was opened, and a hole ~10 mm in diameter was drilled through the layer of acrylic and the bone, exposing the dura.

Neuronal recording and stimulation

During the daily recording sessions, the monkey sat in a Lexan primate chair with the head restrained by the head bolt. A hydraulic microdrive (Narishige) was mounted to the top of the recording chamber. A steel guide tube (an 18-gauge syringe needle) was lowered through the hole in the skull and into the granulation tissue that lay over the dura. The varnish-coated tungsten microelectrode (impedance, 0.5–2 MΩ; Frederick Haer) was advanced from the guide tube through the dura and into the brain. Typically an electrode would start with an impedance of ~2 MΩ. After repeated use on multiple days, as the insulation began to wear off near the tip, the impedance would begin to drop. When clear single neurons were no longer easily isolable on the electrode, a new one was used for the next penetration.

The introduction of the electrode into the cortex was confirmed by monitoring neuronal activity on an oscilloscope and over a loudspeaker. The location of the top of the cortex was estimated as the depth at which spiking neuronal activity was first found. The electrode was typically advanced into the cortex 1–2 mm beyond that depth, and electrical stimulation was tested. On some penetrations, multiple depths were tested, separated by 0.5 mm. When the electrode was advanced beyond the cortex and into the white matter, as indicated by the drop in neuronal cellular spiking, electrical stimulation was no longer tested, and the electrode was retracted. A systematic test of different layers of cortex was not attempted in this experiment. In previous experiments (Graziano et al. 2002a), we found that the movement evoked by 500-ms stimulation is similar as the electrode is advanced perpendicularly through cortex and that the movement thresholds are typically lower in the deeper layers of cortex.

At each cortical site studied, stimulation was applied by an S88 stimulator and two SIU6 stimulus isolation units (Grass, West Warwick, RI). Stimulation consisted of a train of biphasic pulses presented at 200 Hz. In some cases, 100, 150, and 250 Hz were also tested, causing similar effects (see RESULTS). Each stimulation pulse had a negative followed by a positive phase; each phase was 0.2 ms in duration. In some cases, phases of 0.4 ms were also tested. For most movements, a 500-ms stimulation train was used.

Current was measured by the voltage drop across a 1-KΩ resistor in series with the return lead of the stimulus isolation units. For each site, we varied the current until an evoked movement was observed. The threshold, the current at which any visible movement was evoked 50% of the time, was determined by two observers. These threshold measurements were thus approximate. The average threshold measured in this fashion was 19 ± 14 (SD) μA . Thresholds were generally lowest (sometimes as low as 5 μA) in the anterior bank of the central sulcus. For quantification of the evoked movement, the current was usually set between 25 and 100 μA . The current level was

adjusted until a clear, consistent, multijoint movement of the arm was obtained, and the quantitative testing was begun.

Asanuma and Arnold (1975) found that extended trains of cathodal pulses killed the cortical tissue around the electrode tip. With balanced biphasic pulses, however, it is possible to stimulate for long durations (seconds) and high currents (milliamperes) without measurable damage (e.g., Tehovnik 1996). Our stimulation parameters are within the range for cortical stimulation studies in oculomotor, visual, and somatosensory systems (e.g., Bruce et al. 1985; Freedman et al. 1996; Gottlieb et al. 1993; Romo et al. 1998; Salzman et al. 1990; Tehovnik and Lee 1993). To check whether the current damaged the brain, for each site studied, after stimulating for many trials, we switched the amplifier to neuronal-recording mode and confirmed that normal neuronal spiking activity could still be obtained. Second, as Asanuma and Arnold (1975) pointed out, electrical damage to the brain causes the effect of the stimulation to disappear after several trials. We found that the stimulation had a consistent effect over hundreds of trials with no sign of degradation. Finally, in past experiments using the same stimulation techniques (Cooke et al. 2003; Graziano et al. 2002a), on histology we found no visible damage to the cortex associated with the stimulation sites. These lines of evidence suggest that our trains of biphasic pulses do not cause extensive cell death, although more subtle damage cannot be ruled out.

Location of stimulation sites

The monkeys were not killed at the termination of this experiment, thus the locations of the stimulation sites were reconstructed through nonhistological means. The central and arcuate sulci were located first by shining a bright light on the dura during the initial craniotomy surgery. Both sulci were clearly visible through the dura. The microdrive was mounted to the recording chamber, and the locations of the visualized sulci were measured with the tip of the guide tube. In this way, the locations of the sulci were obtained in microdrive coordinates. The sulcus locations shown in Fig. 10 are based on this procedure.

After the craniotomy surgery, during the daily experiments, the measured location of the central sulcus was confirmed to within 0.5 mm by recording and stimulating to either side of the sulcus. Just posterior to the sulcus, in primary somatosensory cortex, we observed the expected small tactile receptive fields on the contralateral hand and also the expected lack of effect of electrical stimulation. Just anterior to the sulcus, we obtained the expected low stimulation thresholds in primary motor cortex. In monkey 2, the location of the arcuate sulcus was confirmed by stimulating just anterior to it and obtaining no skeletomotor movements, but instead obtaining stimulation-evoked saccadic eye movements presumably in the frontal eye fields. The locations of both the central and arcuate sulci were further verified by using the pattern of cellular activity and silence obtained on long electrode penetrations to reconstruct the arrangement of cortex and white matter.

Within the precentral gyrus, the studied area encompassed the arm and hand representation and was bracketed laterally by the face representation and medially by a leg representation. At the most lateral sites shown in Fig. 10, stimulation sometimes evoked movements of the arm, hand, and mouth. Sites that were even more lateral (data not shown) appeared to be in the orofacial region of motor cortex; no arm or hand movements were evoked from these more lateral sites, only facial or oral movements. At the most medial sites shown, stimulation evoked movements of the arm, hand, and leg.

The medial-lateral, anterior-posterior, and dorsal-ventral location of every tested site was supplied to a mapping program to construct a 3-D model of the cortical area studied. The model was flattened, collapsing sites onto a 2-D surface and unfolding the anterior bank of the central sulcus. The plots in Fig. 10 show these 2-D reconstructions, including the gyral surface between the arcuate and central sulci and the unfolded anterior bank of the central sulcus.

Measurement of limb position

To study the effect of different starting postures, stimulation was applied while the monkey performed a simple untrained reaching task. A small piece of fruit was held with forceps by the experimenter at one of many possible locations around the monkey, and the monkey reached for the fruit. On approximately two-thirds of the reaches, stimulation was applied by the experimenter as the hand approached the target location to within about 1 cm but before the monkey had grasped the fruit. The purpose was to stimulate at a moment when the hand was relatively still and at a variety of locations in the workspace and to do so in a manner that did not entrain the monkey to particular postures. Stimulation was also applied during the monkey's spontaneous reaches that placed the hand in different locations in the workspace, and while the monkey was sitting quietly with the arm stationary. In this way, stimulation could be tested during a range of initial postures of the limb. All stimulation trials, whether they took place during a reach to a fruit reward, during spontaneous reaches, or when the monkey was resting, were combined in the data because the resultant stimulation-evoked movement of the arm to a final posture was similar for all of these cases. Data were collected continuously during a 3-min block in which an average of 25 stimulation trials were tested. Two to three blocks were tested for each stimulation site.

The positions of points on the limb were measured by means of an Optotrak 3020 system (Northern Digital). This system tracks the 3-D position of infrared light emitting diodes (LEDs). Each LED could be separately tracked to a spatial resolution of 0.1 mm. The position was measured every 14.3 ms. To create a marker that could be detected by the Optotrak cameras from any angle, we glued five individual LEDs together to produce an omni-directional marker ball. A marker ball was taped to the monkey's forefinger on the dorsal surface where it would not interfere with grasping; on the thumb, again on the dorsal surface where it would not interfere with grasping; on the back of the hand, between the knuckles of the third and fourth digits; on the lateral aspect of the elbow; and on the shoulder. In addition, 14 individual markers were taped in a double ring around the monkey's wrist, with 7 markers per ring and a 1-cm spacing between the rings. A marker was also taped to the monkey's lower jaw to measure the opening and closing of the mouth and to measure the relative position of the hand and face. A marker was taped to the side of the primate chair to calibrate the position of the monkey with respect to the chair. For the LEDs attached to the arm and hand, the wires were taped in a bundle to the underside of the arm and draped behind the monkey. The monkey's chair was open at the front and side, allowing for almost total range of movement of the arm. The monkey's other arm, ipsilateral to the stimulating electrode, was not studied with Optotrak markers. To ensure that this hand would not reach for the fruit rewards during trials or tear off the markers taped to the measured hand, this untested hand was fixed to the side of the chair in an arm holder.

The marker balls on the index finger and thumb were used to measure grip aperture. The marker ball on the back of the hand was used to measure hand position.

The double ring of 14 markers around the wrist was subject to a rigid body computation to calculate the center point and spatial orientation of the wrist. In this computation, for each time-point, a 3-D rigid model of the double ring of markers was fitted to the measured positions of the currently visible markers, using a least-squares method of optimal fit. The orientation and position of the model could be used to estimate the orientation and center of the wrist. The center of the wrist was taken to be the mean position of the 14 points in the model.

Once the orientation and position of the wrist was calculated, the elbow position in space could be calculated by assuming that the elbow was a certain distance from the center of the wrist in a direction specified by the orientation of the wrist. This calculation required knowing the distance between the elbow and the wrist markers; this reference distance was measured each day after the ring of markers

was put on the wrist and was typically about 12 cm. The calculated spatial position of the elbow, derived from the wrist markers, was consistently 1–2 cm medial to the marker that was fixed to the lateral aspect of the elbow, as expected. The calculated position was assumed to be closer to the actual point of rotation of the elbow, internal to the arm. For this reason, in reconstructing the posture of the arm, this calculated elbow position was used rather than the location of the marker on the surface of the elbow.

The position of the shoulder in space was calculated by analyzing the position of the elbow over time. Over many time-points, the elbow described a portion of a sphere, the origin of which was located at the shoulder joint. For each 3-min block of data, a shoulder position was calculated by fitting a sphere to the data using a least-squares best-fit algorithm and using the center of the sphere as the shoulder location. Because the shoulder is capable of small translational movements in addition to rotations, this method of estimating shoulder joint location is approximate but was sufficient for the purposes of this study. When the shoulder position was calculated multiple times over different time segments, it varied within <3 cm. Just as for the elbow, the calculated position of the shoulder joint was assumed to be more accurate than the measured position of the marker ball fixed to the shoulder. The calculated position was at the actual point of rotation, as estimated by the best fit algorithm, whereas the marker ball was fixed to the lateral surface of the shoulder. Thus in reconstructing the posture of the arm, the calculated shoulder position was used.

Three shoulder angles were computed: the elevation; the azimuth; and the "twist" or internal/external rotation of the shoulder joint. We also calculated the flexion of the elbow; the pronation of the forearm; the extension of the wrist; the adduction of the wrist; and the grip aperture. In total, eight degrees of freedom were calculated for the arm. This model of the arm was verified by applying forward kinematics to estimate the position of the hand. This calculated position of the hand matched the actual, measured position of the hand to within an accuracy of 1.5 cm.

Testing the effect of a weight on the arm

On some blocks of trials, a 90-g lead bracelet was wrapped tightly around the contralateral wrist just proximal to the ring of Optotrak markers. A 90-g weight represents about 2% of body weight or about 25% of arm weight (arm weight ~ 300 g). In pilot tests using heavier weights such as 130 g, the monkey was unwilling to lift its hand, and therefore we were not able to test different initial hand locations. In contrast, with the 90-g weight, the monkey did reach for fruit rewards and thus we could test a range of initial locations.

For each stimulation site, we first tested the stimulation-evoked movement without a weight on the wrist in a 3-min block of stimulation trials (typically 25 trials). Then the weight was added, and a second block of trials was run. This alternation of unweighted and weighted blocks was continued, typically for four to six blocks.

To help test whether the system showed any evidence of compensation for the weight, we estimated the expected effect that the weight should have if there was no compensation. To perform this calculation, we modeled the physics of the arm. The model involved two hinged segments: an upper arm and a forearm. The shoulder had three degrees of freedom of rotation, and the elbow had one degree of freedom. The model incorporated the gravitational force on these segments, a spring-like muscle force acting around each degree of joint rotation, and a damping term for each degree of joint rotation. Note that this type of model is deterministic; given the lengths and weight distributions of the segments, the force of gravity, and the spring constant, equilibrium angle, and damping force for each joint, Newtonian mechanics fully specifies the equations of motion. We used the Denavit-Hartenberg representation, a standard method for simplifying the equations of a multilink arm (Denavit and Hartenberg 1955), and the recursive Newton-Euler method, a standard method to transform between kinematic variables and dynamic variables in a

multilink arm (Luh et al. 1980; Walker and Orin 1982). The lengths of the arm segments were taken directly from the Optotrak measurements of the arm. Each segment was approximated as a cylinder of uniform width and density. The diameter of each segment was taken as the approximate mean diameter of the monkey's arm (6 cm). The total arm weight was set to 300 g, which matched our estimate from volumetric measures of the arm. Each degree of freedom of joint rotation was modeled as a spring system and given a spring constant, an equilibrium angle, and a damping term. These parameters were different for different stimulation sites. They were determined in the following way. For each stimulation site tested, we analyzed the data collected from the arm on actual trials when no weight was present. We used the joint angles, angular speed, and angular acceleration, and applied a least-squares method of optimal fit to estimate the spring constants, equilibrium angles, and damping terms that best characterized the movement for those trials. We incorporated those dynamic terms into the model. Using the model, we were able to obtain simulated trajectories that closely matched the real trajectories.

We ran the model with an added 90-g weight on the wrist and obtained the calculated trajectory and final position of the hand. This calculation showed, as expected, that the weight should have two principal effects: because of the increased inertial mass, it should reduce the peak acceleration of the movement, and because of the greater downward gravitational force on the hand, it should cause the final height of the hand to be lower. These effects predicted by the model were always pronounced because of the fact that that weight was concentrated at the wrist. We compared this calculated effect of the weight to the actual data collected with the weight fixed to the wrist. This comparison is detailed in RESULTS.

RESULTS

Stimulation-evoked hand trajectories: basic description

Hand trajectories were measured during electrical stimulation of 91 sites in motor cortex. Figure 1 shows examples of hand trajectories evoked by stimulation of 18 typical sites. In each case, stimulation evoked a movement of the arm toward a final posture, and thus a movement of the hand toward a final region of space. As can be seen across the 18 examples, stimulation of different sites in cortex drove the hand toward different spatial regions.

Was the convergence of the hand to a location caused by the stimulation, or was the monkey somehow cued by the context to perform a learned movement? While testing the stimulation site shown in Fig. 1*S*, after evoking a convergence of the hand toward a final location, we disconnected the stimulator from the electrode and tested sham stimulation. The results are shown in Fig. 1*T*. The sham stimulation, just like the actual stimulation, was applied as the hand neared a fruit reward but before the monkey grasped the reward. Some hand movement was observed during sham stimulation, but this movement was minimal and was often directed in a divergent fashion, away from central space, consistent with the hand continuing its trajectory toward the fruit reward. The pattern obtained during sham stimulation was therefore unlike the pattern obtained during actual brain stimulation at that site and unlike the pattern found at any stimulation site.

Figure 2*A1* shows speed profiles for a typical stimulation site. To calculate latency, we fit a straight line to the prestimulation baseline data using a least-squares fit, fit a straight line to the rising phase of the speed, and determined the time at which the two lines intersected. Calculated in this fashion, the latency was 82.4 ms. (The average latency among the 91 sites was 80.2 ± 10.9 ms, with a range of 49.9–103.3 ms).

The speed profiles were usually bell-shaped. This bell-shaped property can be seen more clearly in Fig. 2*A2*. Here, the same trials are aligned on peak speed. This example site shows a statistically significant fit to a Gaussian curve (regression analysis, $F = 405$; $P < 0.0001$). This fit to a Gaussian was statistically significant for all 91 sites (significance level of 0.05, Bonferroni-adjusted for 91 tests).

Figure 2*A3* shows the peak speed as a function of the distance that the hand traveled. The relationship is roughly linear, in which greater peak speeds occurred during longer movements. For this example site, the data show a significant linear trend (regression analysis, $F = 235$; $P < 0.0001$). A significant linear trend was obtained for 90 of the 91 sites tested (significance level of 0.05, Bonferroni-adjusted for 91 tests).

Figure 2, *B* and *C*, shows similar results for two more example sites.

We typically tested sites using 200-Hz stimulation, a frequency borrowed from the oculomotor literature (e.g., Robinson and Fuchs 1969). For six cortical sites, we examined the effect of different frequencies. Figure 3 shows the results for one site tested with stimulation at 100, 150, 200, and 250 Hz. The movement of the hand was similar across these different stimulation frequencies. In each case, the hand converged from a range of initial positions toward a similar final region of space. As shown in Fig. 3*E*, the peak speed of movement varied somewhat with stimulation frequency. The lowest speeds were obtained with 100-Hz stimulation; the highest speeds were obtained with 200- and 250-Hz stimulation. This effect of stimulation frequency on hand speed was significant ($F = 15.53$; $P < 0.0001$). These results suggest that similar movements can be evoked with a broad range of stimulation frequencies, although higher frequencies tended to evoke somewhat higher speeds.

Convergence of the hand toward a location

The most consistent feature of the stimulation-evoked movements was the convergence of the arm toward a posture, and thus the convergence of the hand toward a region of space. This convergence can be seen in the 18 example sites depicted in Fig. 1. Figure 4*A* shows this convergence in greater detail for a typical site. The convergence of the hand is shown in each of the three Cartesian dimensions. To study the degree of convergence further, we calculated the "mean-distance-to-center" and analyzed how this metric evolved over time during the stimulation. The mean-distance-to-center is a measure of dispersion around the mean. For each time increment, we first calculated the mean hand position across all trials. Then, for each trial, we computed the radial distance from the hand to that mean position. Finally, we averaged these distances across trials to arrive at the mean-distance-to-center.

Figure 4*A4* shows that, for this example site, the mean-distance-to-center began at a high level and dropped during stimulation. This drop in mean-distance-to-center began about 80 ms after the onset of stimulation. It is important to note that this 80 ms is not simply the latency for the hand to move. Rather, it is the latency with which the hand began to converge toward a tighter cluster of locations. To determine if the degree of convergence was statistically significant, we compared the mean-distance-to-center at the start of stimulation and at the end of stimulation (paired *t*-test). The mean-distance-to-center was significantly reduced at the end of stimulation ($t = 14.58$;

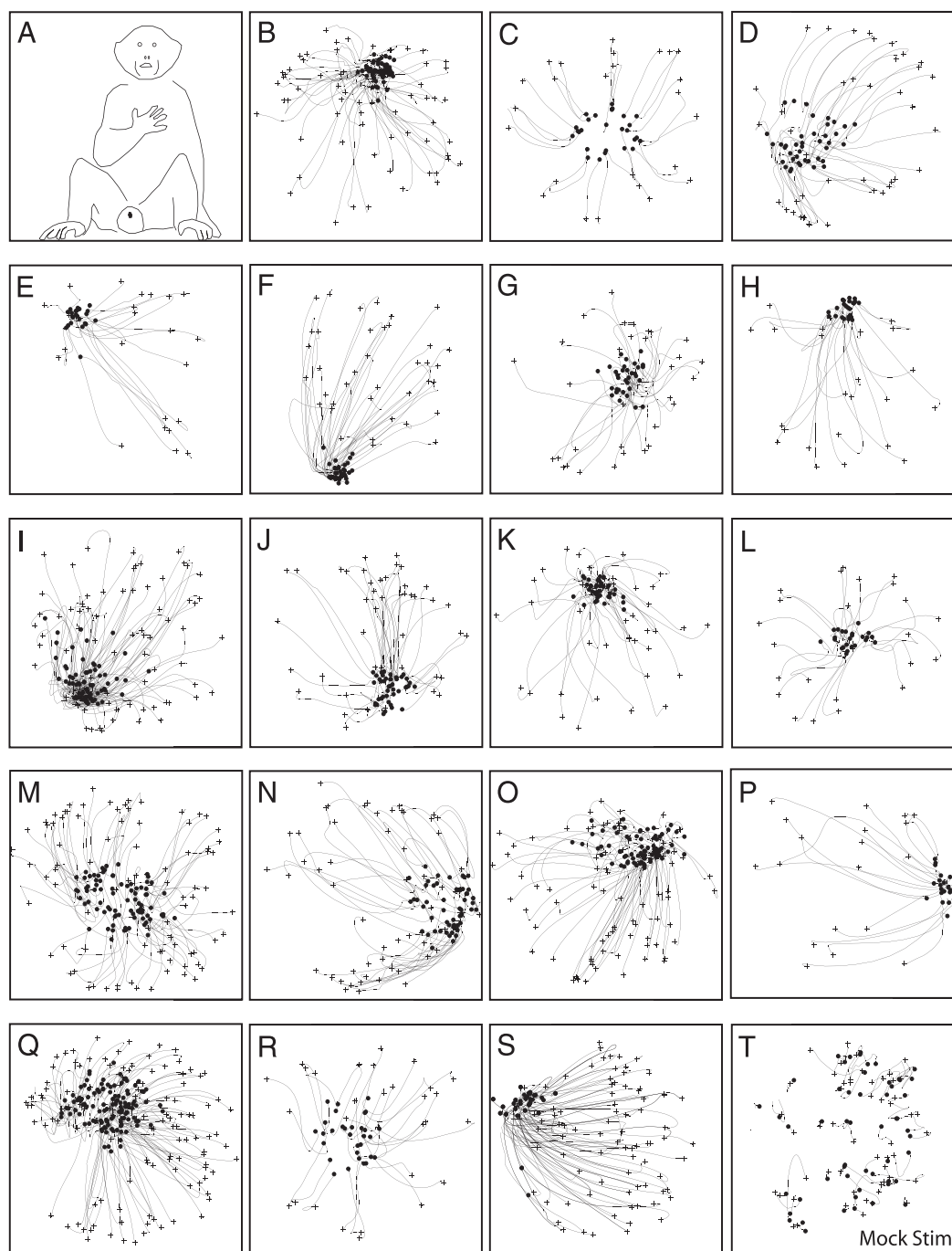


FIG. 1. Examples of hand movements evoked by microstimulation in motor cortex. *A*: monkey drawing indicates approximate size, location, and perspective of the monkey within the square frame. Height of frame represents 50 cm. *B–S*: stimulation-evoked hand movements from 18 typical stimulation sites. Each thin black line shows path of the hand during a stimulation train. +, start of movement. Black dot indicates end of movement. In a small number of trials, tracking markers were transiently blocked from view of the camera because of the specific posture of the limb. In these cases, the trace is interrupted. *T*: result of mock stimulation in which wires to the electrode were disconnected but all other aspects of testing were the same. Traces in *S* show result for this same cortical site when the wires were connected.

$P < 0.0001$), indicating that the stimulation caused a significant spatial convergence.

Figure 4, *B* and *C*, shows similar results for two more example sites. These examples are typical of the population. Of the 91 sites tested, all 91 showed a statistically significant degree of convergence of the hand (significance level of 0.05, Bonferroni-adjusted for 91 tests).

Figure 4*D* shows the mean result for all 91 sites tested. Just as for the individual examples, for the group data, the mean-

distance-to-center began to drop after stimulation, and the latency of this drop was ~ 80 ms.

Effect of a weighted bracelet on the final stimulation-evoked height of the hand

As shown above, for almost all cortical sites, stimulation caused the hand to converge from any initial position toward a final region of space. How is this final position affected by a

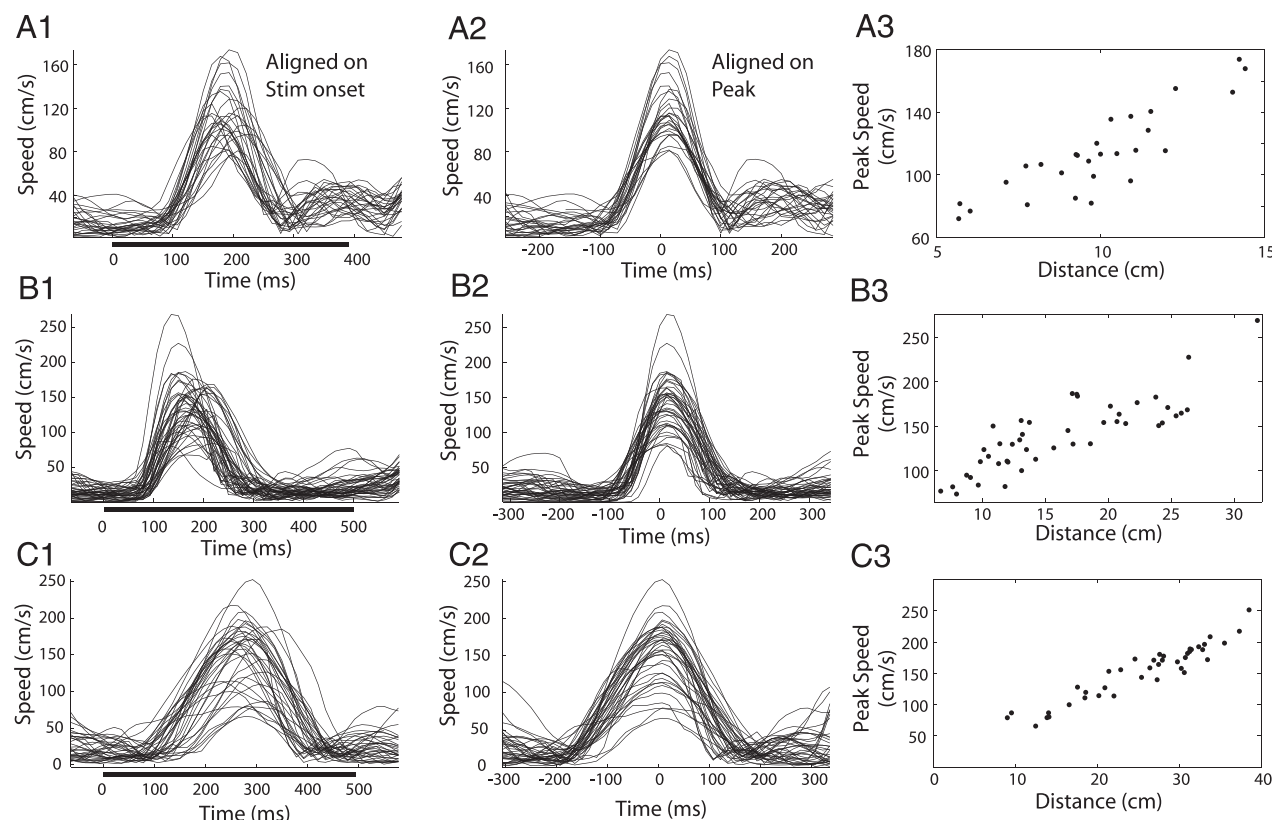


FIG. 2. Speed profiles for 3 typical stimulation sites. *A1*: hand speed as a function of time during stimulation for 1 stimulation site. Each trace shows result for 1 stimulation trial. Speed measured in 14.3-ms increments. Thick black bar at *bottom* shows time of stimulation. *A2*: same data as in *A1* but traces are aligned on time of peak speed. *A3*: peak speed during stimulation-evoked movement as a function of distance that the hand traveled. *B* and *C*: similar plots for 2 more stimulation sites.

weight fixed to the arm? We tested sites by fixing a 90-g lead bracelet to the wrist ($\sim 25\%$ of arm weight).

WAS THE PEAK ACCELERATION SIGNIFICANTLY REDUCED BY THE WEIGHT? Each stimulation site was analyzed in the following manner. For each trial, we found the peak acceleration of the hand during the stimulation-evoked movement. We averaged across trials to obtain the mean of the peak accelerations. We compared this mean peak acceleration between the weighted and unweighted trials. Figure 5 shows group data for the 50 stimulation sites tested. In general, the peak acceleration was lower when the weight was present (binomial test, $P < 0.0001$). This finding shows that the weight was sufficiently large to measurably reduce the acceleration of the hand during stimulation.

WAS THE FINAL POSITION OF THE HAND SIGNIFICANTLY LOWERED BY THE WEIGHT? Figure 6A shows data from one example site. Figure 6A1 shows trials in which no weight was fixed to the

arm, and Fig. 6A2 shows interleaved blocks of trials in which the hand was weighted with the 90-g lead bracelet. In both conditions, the hand stabilized at a similar final height by the end of stimulation. Thus the weight did not appear to have a pronounced effect on the final, stimulation-evoked height of the hand, for this particular stimulation site.

We further analyzed the results by examining how the weight affected the position of the hand at different time-points throughout the stimulation trial. For each time-point, we calculated the mean difference in height between the weighted condition and the unweighted condition. This time-course is plotted in Fig. 6A3. At the start of stimulation, the mean height of the hand was approximately the same for both weighted and unweighted conditions (a difference of ~ 0). As the stimulation progressed, the weight began to affect the hand compared with the unweighted condition. This difference reached a maximum about 300 ms after the start of stimulation, at which time the

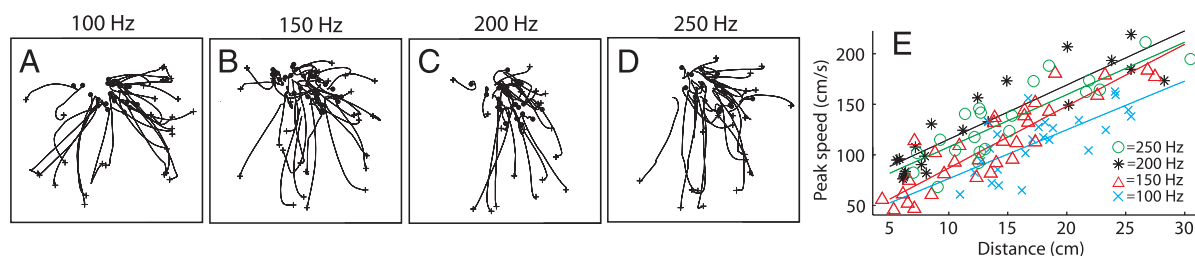


FIG. 3. Effect of different stimulation frequencies on evoked hand movement for 1 stimulation site. *A–D*: movement of the hand evoked by stimulation at 100, 150, 200, and 250 Hz. See caption to Fig. 1 for details of movement traces. *E*: peak speed of movement vs. distance that the hand moved for the 4 different stimulation frequencies.

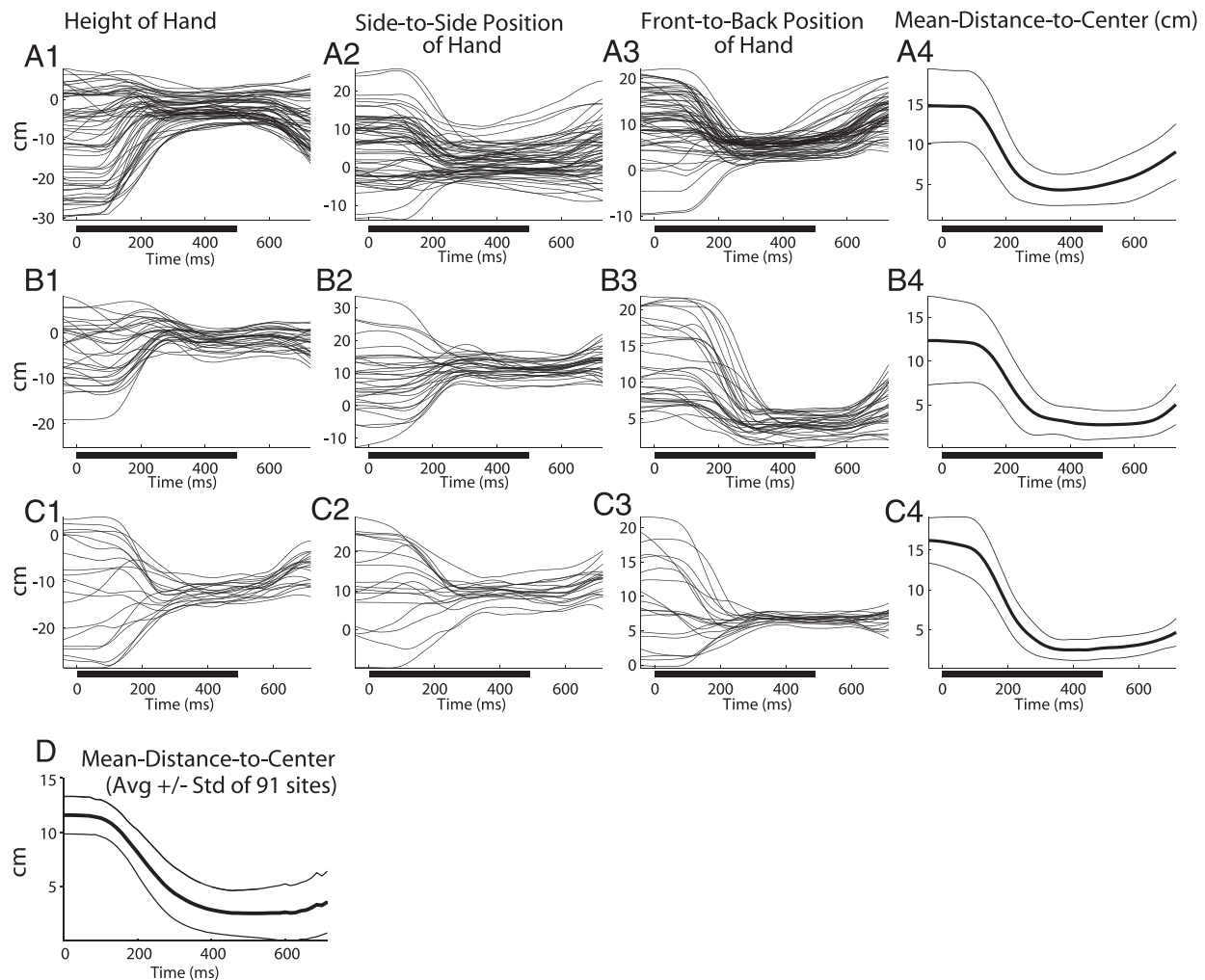


FIG. 4. Stimulation-evoked convergence of the hand. A1: height of the hand as a function of time during stimulation of a typical cortical site. Each line shows data from 1 stimulation trial. Thick black bar at bottom indicates time of stimulation train. Height of 0 indicates height of mouth. A2: data from same stimulation site showing side-to-side position of the hand. Mouth at 0. Negative numbers indicate positions behind level of mouth; positive numbers indicate positions in front of level of mouth. A3: data from same stimulation site showing front-to-back position of the hand (position along the monkey's line of site). Mouth at 0. Negative numbers indicate positions behind level of mouth; positive numbers indicate positions in front of level of mouth. A4: mean-distance-to-center (measure of spatial dispersion) \pm SD for this same example site. B and C: similar plots for 2 more stimulation sites. D: group data for 91 sites. Mean and SE mean-distance-to-center.

hand was on average 1.7 cm lower in the weighted condition than in the unweighted condition. This effect of the weight began to diminish. By the end of stimulation, the height of the hand was once again similar for the weighted and unweighted condition. Thus the weight did affect the movement of the hand during the trial, but by the end of the stimulation train, the weighted hand had reached the same height as the unweighted hand.

We tested whether the effect of the weight on the final height of the hand was statistically significant in the following manner. We first plotted the final height of the hand (at time 500 ms, the end of stimulation) against the initial height of the hand (at time 0 ms, the start of stimulation). This plot is shown in Fig. 6A4. We then used an analysis of covariance, in which the initial height of the hand was the covariant variable, the final height of the hand was the dependent variable, and the presence or absence of the weight was the independent variable. In this example, the final height of the hand was not significantly different for the weighted and unweighted conditions ($F = 0.001$; $P = 0.971$). Thus for this particular stimulation site, the

hand moved to a similar final height regardless of whether the weight was present or absent.

Figure 6B shows similar data from another example site for which the weight did not significantly affect the final height of the hand. Figure 6C shows data from a stimulation site for which, unlike the previous two examples, the final position of the hand was significantly reduced by the weight.

A total of 50 stimulation sites were tested with and without a weight fixed to the wrist. For each stimulation site, we calculated the mean distance that the hand was dragged down by the weight at the end of the stimulation train. We calculated whether this effect of the weight was significant using an analysis of covariance as outlined in the examples above. We plotted this data on a frequency histogram, shown in Fig. 6D. Of the 50 sites, 13 (26%) showed a significant drop in hand height caused by the weight, and 37 (74%) did not (significance level of 0.05, Bonferroni-adjusted for 50 tests). No sites showed a significant increase in hand height caused by the weight. We also found that no sites showed a significant horizontal shift of hand position because of the weight. Be-

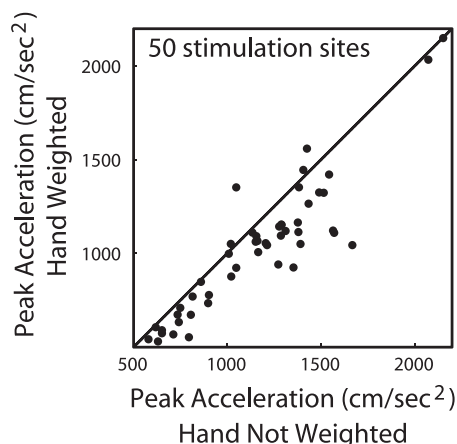


FIG. 5. Effect of a weighted bracelet on the acceleration of the hand. For each stimulation-evoked movement, peak acceleration was found. Peak accelerations for different trials were averaged to find mean peak acceleration. Mean for weighted condition (with 90-g lead bracelet) was plotted against mean for unweighted condition. Each dot shows mean from 1 stimulation site. Almost all data points are below the $y = x$ line, indicating that acceleration was smaller when weight was present. Thus weight was heavy enough to cause a measurable effect on movement of the hand.

cause the weight adds only a vertically downward component of force, a systematic horizontal shift in hand position was not expected. There was no clear topography of sites that showed an effect of the weight and sites that did not; both types of sites were intermingled in cortex. There was also no clear distinction between the types of evoked movements that compensated for the weight and those that did not. There was a trend for final hand positions that were far from the body, with the arm outstretched, to show a smaller effect of the weight (greater compensation). This correlation between hand distance from body and effect of the weight did not reach significance (mean difference between weighted and unweighted final height vs. mean final distance of the hand from the chest; $r = 0.19$; $F = 1.82$; $P = 0.184$).

WAS THE FINAL POSITION OF THE WEIGHTED HAND HIGHER THAN THE PREDICTED POSITION? One potential concern with the above test is that the weight may be too small to have a reliable effect on the height of the hand, whether or not compensation is present. We used a mathematical model to approximate the expected effect of a 90-g weight on the movement of the arm, assuming no compensation for the weight. We modeled the physics of a two-link arm with three degrees of freedom of shoulder rotation and one degree of freedom of elbow rotation. The model incorporated spring-like muscle forces, damping forces, gravitational forces, and the inertia tensor of the two-link arm. The model is approximate; it provides a rough estimate of the expected effect of the weight, which can be compared with the actual effect of the weight.

Figure 7, A–D, shows the results of this analysis for one example site. Figure 7A shows the measured, actual trajectories of the hand when no weight was present. We used the data from these trials including joint angle, angular speed, and angular acceleration, and applied a least-squares method of optimal fit to estimate the spring constants and damping terms that best characterized the movements during these trials. We incorporated those dynamic terms into the model. Figure 7B shows the simulated trajectories obtained from the model, using the same initial positions and speeds as in the actual

trials. The model closely matched the actual data, indicating that the fit algorithm was successful. Figure 7C shows the measured, actual trajectories of the hand when the weight was added to the hand. Again, the hand converged on approximately the same final height. In this case, the weight appeared to affect the hand initially, pulling it to a slightly lower position, but in the second half of the trial, the hand rose up to a similar final height as without the weight. The mean final height of the hand was 0.4 cm higher in this weighted condition (Fig. 7C) than in the nonweighted condition (Fig. 7A). We ran the model with an added 90-g weight on the wrist and obtained the calculated trajectories of the hand, shown in Fig. 7D. In the model, the hand converged to a position that was on average 5.8 cm lower than in the actual data. This site is typical in that the model predicted a pronounced effect of the weight.

We compared the data from Fig. 7, C (measured data with weight added) and D (simulated data with weight added), using an analysis of covariance. The initial height of the hand was the covariant variable, and the final height of the hand was the dependent variable. The final height of the hand was significantly higher in Fig. 7C than in Fig. 7D ($F = 73.4$; $P < 0.0001$). Thus there is evidence of an active compensation for the weight, in that the electrical stimulation lifted the hand to a significantly greater height than was estimated if no compensation were to occur.

A total of 50 stimulation sites were tested in this fashion, and 47 (94%) showed a significant difference (significance level of 0.05, Bonferroni-adjusted for 50 tests). For these sites there was evidence of active compensation for the weight. For three sites (6%), however, the weighted hand was not lifted significantly higher than estimated for the case of no compensation.

Movement of individual joints

To probe the movement of the limb to a posture in greater detail, we measured the angles of joints in the arm and the grip aperture. Figure 8A shows the results for one stimulation site. Eight graphs are shown, corresponding to the eight degrees of freedom that were measured. During stimulation, the joints rotated from a disparate range of initial angles to a more restricted range of angles. For some joints, such as the elbow, the rotation was to an intermediate angle. When the elbow joint was initially flexed, stimulation caused it to extend toward the final angle; when it was initially extended, stimulation caused it to flex toward the final angle. For other joints, such as the shoulder azimuth, the rotation was in one direction. For the wrist adduction angle, relatively little range of movement was obtained during stimulation. This wrist angle generally showed little change compared with other joint angles, even during the monkey's spontaneous movements. Figure 8B shows joint angles from another example site.

For each site, we calculated the mean stimulation-evoked angle for each joint. Figure 8C shows a frequency histogram of all sites. A range of angles was represented, including extreme angles and intermediate angles.

Interaction between joints stabilizes the hand for some stimulation sites

One hypothesis is that stimulation independently drives each joint to a specific angle, and as a result of this aggregate of joint

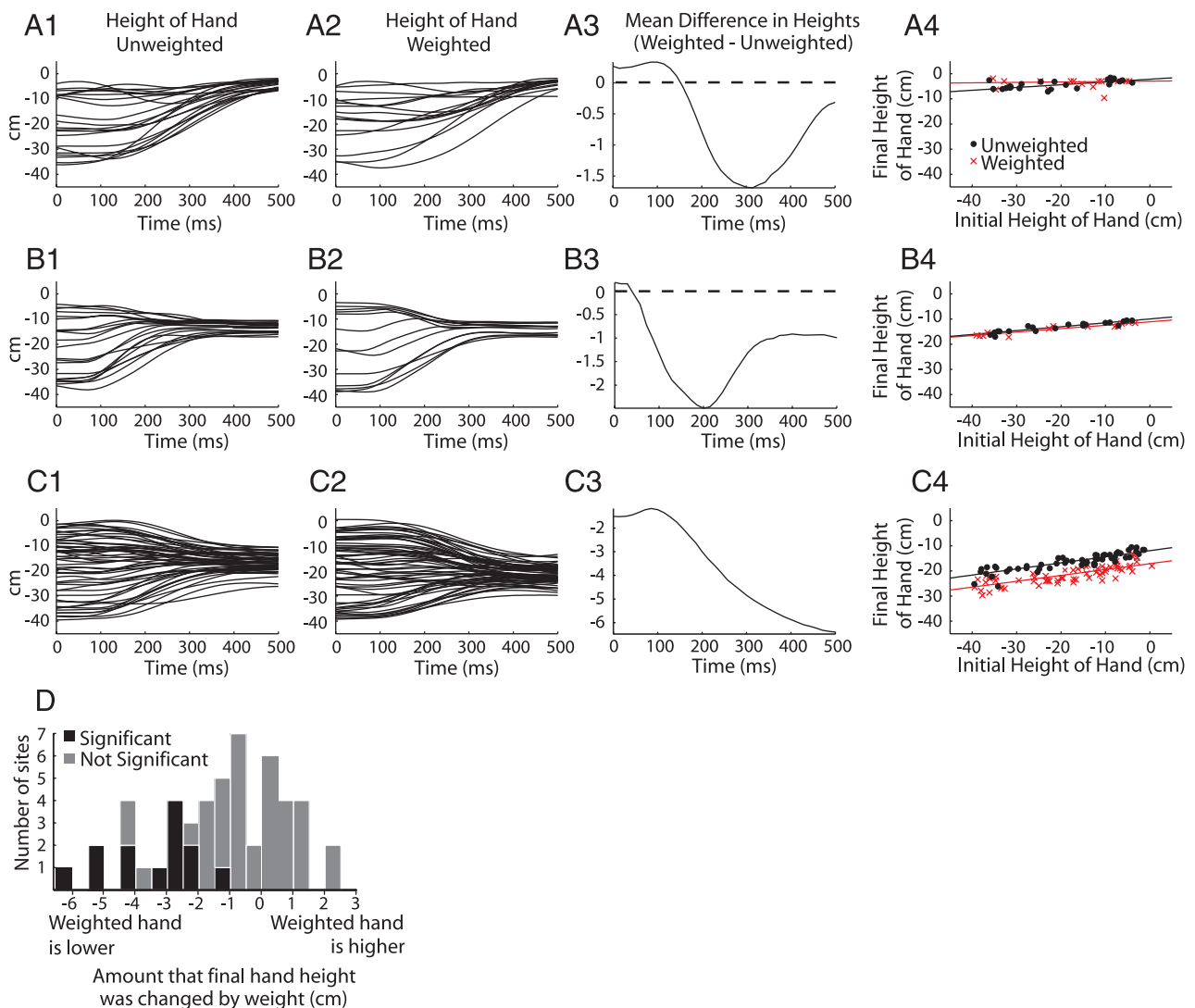


FIG. 6. Effect of a weighted bracelet on height of the hand. *A1*: height of the hand as a function of time during stimulation for a typical site. Stimulation began at time 0 and ended at time 500. Each trace shows data for 1 stimulation trial. No weight was fixed to the wrist on these trials. *A2*: data from the same cortical site when weight was fixed to the wrist. *A3*: difference in mean height when weight was present and when weight was absent. Difference of 0 indicates no change in height caused by weight. Negative difference indicates that the hand was lower when weight was present. *A4*: final height of the hand (at time 500) as a function of initial height of the hand (at time 0). Final height was lower for weighted condition (red crosses) than for unweighted condition (black dots). *B*: similar plots for a 2nd stimulation site. *C*: similar plots for a 3rd stimulation site.

angles, the hand moves to a location in space. Another hypothesis is that the joints move in a coordinated manner, each joint adjusting to compensate for slight deviations in the other joints, to bring the hand more specifically toward

a desired location. We asked whether the trial-by-trial variability in each joint might compensate for the variability in the other joints in a manner that would help to stabilize the hand in space.

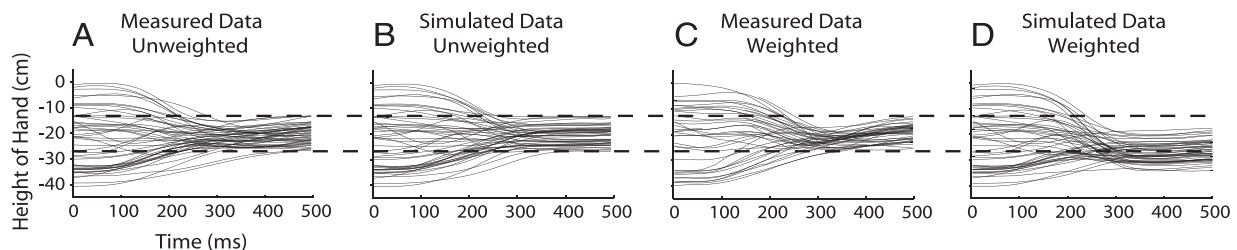


FIG. 7. Estimating the expected effect of a weighted bracelet on height of the hand. *A*: data from an example site. y-axis shows height of hand relative to mouth height; x-axis shows time during stimulation trial. Each trace shows data from 1 trial. Dotted lines show range (min and max) of final heights. *B*: we modeled physics of the arm and used data from trials shown in *A* to find a best fit for spring constants and damping forces in the model. Graph shows calculated trajectories for the model. *C*: data from the same example site as in *A*. On these trials, a 90-g weight was fixed to the wrist. *D*: calculated trajectories based on the model, when a 90-g weight was added to the wrist in the model.

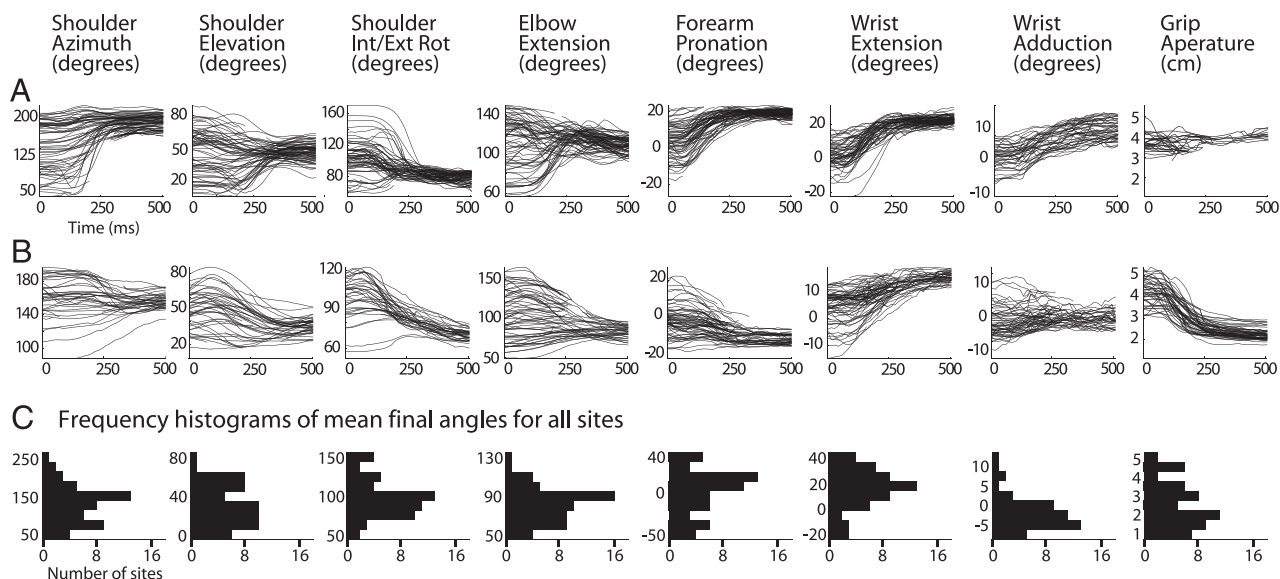


FIG. 8. Tracking 8 degrees of freedom in the arm during stimulation. *A*: results for 1 stimulation site. Each trace shows data for 1 trial. x-axis shows time during stimulation; 0 = start of stimulation, 500 = end of stimulation. y-axis shows joint angle (degrees) or grip aperture (cm). *B*: data from a 2nd example site. *C*: each graph is a frequency histogram showing distribution of mean final angles across 61 stimulation sites tested.

Figure 9A shows the results for one example site. For this analysis, we concentrated on four arm angles: shoulder elevation, shoulder azimuth, shoulder internal/external rotation, and elbow flexion. These arm angles, together with the lengths of the arm segments, define the position of the wrist in space. For each of the 37 trials, using the angles reached at the end of stimulation and applying forward kinematics, we calculated the final position of the wrist. These final wrist positions are plotted as black dots in Fig. 9A.

We randomly “shuffled” the trials in the following manner. A shuffled trial might contain the shoulder elevation angle from trial 1, the elbow flexion angle from trial 16, etc. The rule for a shuffled trial was that none of the four joint angles that composed the shuffled trial had been collected on the same actual trial. In this fashion, 37 randomly shuffled trials were constructed. We used forward kinematics on these shuffled trials to calculate final wrist positions. If the joints seek their final angles independently, shuffling the trials in this manner should have little effect on the result. However, if the joints

normally interact within a trial, such that a slight deviation in one joint is compensated by slight deviations in the other joints, shuffling the trials will remove this interjoint compensation and result in a wider distribution of final wrist positions. As shown in Fig. 9A, the shuffled trials (○) did show a wider distribution of final wrist positions than the actual trials (●). As a measure of the spread of final positions, we used the mean-distance-to-center. For this example site, the mean-distance-to-center for the shuffled trials was 6.03 cm, and the mean-distance-to-center for actual trials was 3.33 cm.

Figure 9A shows only one possible reshuffling of the 37 trials. We tried 40,000 possible reshuffles and for each one calculated a mean-distance-to-center. Figure 9B shows the distribution. The arrow shows the position of the actual data on this distribution. Of the many ways to reshuffle the data, all of them resulted in a greater spread of final hand positions than the actual data ($P < 0.0001$). These results show that, within a stimulation trial, the joint angles were not independent but instead interacted. Deviations in some joints must have been matched by compensatory deviations in other joints in a manner that helped to stabilize the hand at a particular location in space.

A similar analysis was performed for each stimulation site. Of 61 sites tested in this manner, 54% had a significant effect similar to the effect shown in Fig. 9, in which interactions between the joints stabilized the stimulation-evoked hand location (significance level of 0.05, Bonferroni-adjusted for 61 tests). For 46% of the sites, no significant effect of joint interaction was obtained. Thus only approximately one-half of the sites showed this stabilization of the hand in space. There was no clear topography of sites that showed significant joint interactions and sites that did not; both types of sites were intermingled in cortex.

Movement categories arranged in separate cortical zones

Five categories of movements and their locations on the cortex are shown in Fig. 10A.

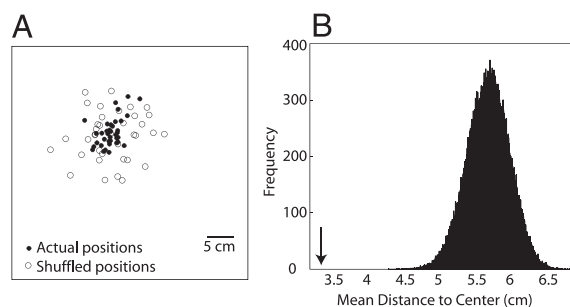


FIG. 9. Interactions between joints stabilized hand position. *A*: data from 1 example site. Black dots show final hand positions for 37 stimulation trials, calculated from measured joint angles. Open circles show final hand positions calculated from 37 “shuffled” trials, using the same data but with joint angles randomly shuffled across trials. *B*: 40,000 different shuffles of 37 trials were tested. For each shuffle, 37 final hand positions were found through forward kinematics, and mean-distance-to-center was calculated (a measure of spatial spread of hand positions). These mean-distance-to-centers were plotted on the frequency histogram shown. Mean-distance-to-center for actual data are indicated by the arrow.

HAND-TO-MOUTH. At some stimulation sites we evoked a characteristic hand-to-mouth movement, defined by the following properties: the grip aperture closed during stimulation as measured by the Optotrak, the hand moved to a location within 1 cm of the mouth as measured by the Optotrak, and the mouth opened.

DEFENSIVE-LIKE. Another cortical zone could be delineated on the basis of the following specialized properties: the neurons responded to tactile stimuli on the face and arms and visual stimuli near or approaching the tactile receptive fields; stimulation evoked defensive-like movements including a blink, squint, lifting of the upper lip in a facial grimace, shrugging of the shoulder, and sometimes a blocking movement of the arm. These defensive-like movements were noted here qualitatively and have been extensively studied in a more quantitative fashion in previous experiments (Cooke and Graziano 2004a,b).

CENTRAL SPACE + FINGER MOVEMENT. A specific type of movement involving both the arm and the hand satisfied the following criteria: the hand moved into a restricted region of space, within 10 cm of a central point in front of the chest (12 cm vertically below the chin); the grip aperture changed, as measured by the Optotrak. Qualitatively, these finger movements resembled an apparent precision grip (thumb against forefinger), a power grip (fist), or a splaying of the fingers accompanied by a turning of the palm toward the face.

REACH. For some cortical sites, the hand moved to a location distant from the body (>10 cm from the central point just in front of the chest), and the grip aperture opened. Subjectively, these movements resembled reaching to grasp.

OTHER OUTWARD ARM MOVEMENTS. At many sites, stimulation drove the hand to a distal location (>10 cm from the central point just in front of the chest) but without evoking any opening of the grip aperture. These movements were not clustered in a single zone but instead were scattered, surrounding the reaching sites and the central space/manipulation sites.

ARM + LEG. In a large medial and anterior region, stimulation evoked movements that combined the arm and leg. Unlike movements evoked from the other regions of cortex, these movements were typically bilateral, sometimes involving all four limbs.

NO EVOKED MOVEMENT. In monkey 1, in an anterior region of cortex, stimulation did not evoke movements even when the current was raised to 300 μ A.

Topography of hand location across the cortical surface

Figure 10B shows one type of topography involving hand position. The stimulation sites were categorized according to the proximity of the hand to a central point just in front of the chest, 12 cm vertically below the chin. Sites for which the hand moved into the region of space within 10 cm of this central point were clustered in a posterior region that extended partly onto the bank of the central sulcus. As described above, for almost all of these sites, the fingers also shaped in a specific manner. Sites for which the hand moved outside of this central region were scattered over the remainder of the cortical area.

Figure 10C shows another dimension of topography with respect to hand position. The sites were categorized according

to their vertical position into three spatial regions separated by 16 cm: high (crosses), middle (open circles), and low (closed circles). The most lateral part of the arm representation was dominated by hand locations in upper space. For electrode penetrations that were more medial along the central sulcus, the hand locations were usually in mid-level space, including hand locations in front of the chest. In the most medial sites along the central sulcus, stimulation sometimes drove the hand into lower space. When the electrode entered a medial and anterior region where both the leg and the arm were represented, the organization was less clear, with hand positions in upper, middle, and lower space intermixed.

We tested the statistical significance of the progression of hand heights along the central sulcus as follows. For each site not within the medial, leg-and-arm representation, we calculated the location of the site as projected onto a line that ran along the central sulcus. We used an ANOVA to compare the distributions along this line. The separation was statistically significant between upper and middle hand positions ($P < 0.0001$) and also between middle and lower hand locations ($P < 0.0001$). It is important to point out, however, that although the mapping of hand height along the central sulcus is statistically significant, it is also noisy and contains overlap.

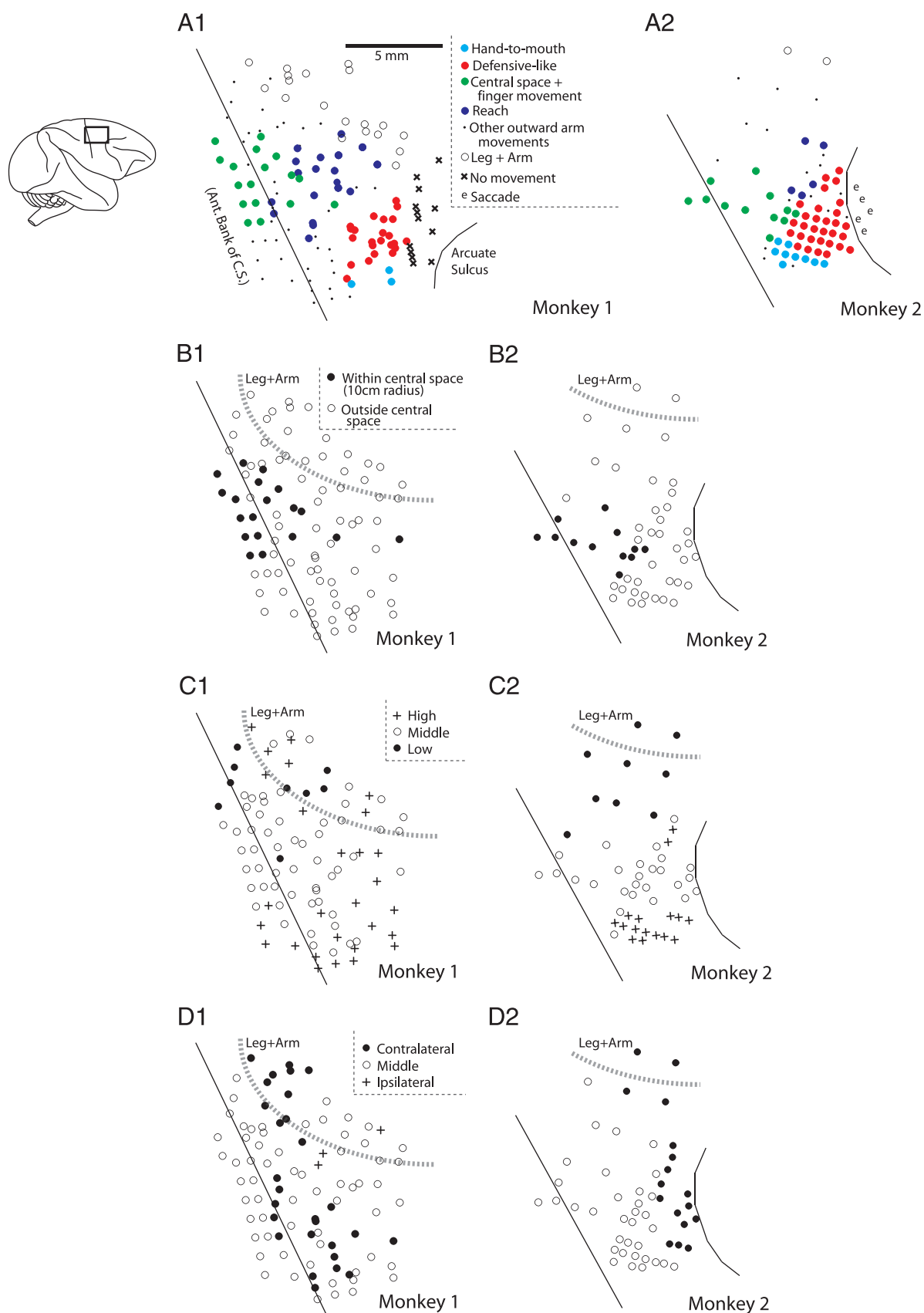
We examined other spatial parameters but found no other consistent topography. Figure 10D shows the distribution of hand locations in a lateral dimension (contralateral, central, and ipsilateral to the electrode). In monkey 1, some clustering but no overall topography is apparent. In monkey 2, some possible topography can be seen in which lateral hand positions were found more anteriorly and central hand positions were found more posteriorly.

DISCUSSION

These experiments examined the arm movements evoked by electrical stimulation in motor cortex using half-second stimulation trains. The movements had a consistent latency of ~80 ms. They generally followed a bell-shaped speed profile in which the peak speed covaried with movement distance, similar to the profiles of natural movements (e.g., Bizzi and Mussa-Ivaldi 1989; Flash and Hogan 1985). Stimulation with different frequencies had a similar effect, although higher frequencies were usually associated with slightly faster movements. Stimulation moved the arm from any initial position toward a final position. This convergence began with a latency of about 80 ms, suggesting that as soon as the arm began to move, it was already directed in a coherent fashion toward the final position. During mock stimulation, when the wires were disconnected from the electrode, these movements did not occur.

Complex, multijoint movements

The central finding from the microstimulation of motor cortex on a behavioral time scale is the production of complex, multijoint movements that resemble actions in the monkey's natural behavioral repertoire. The fact that the movements are multijoint is consistent with the known complexity of the mapping between motor cortex and muscles. A point in motor cortex can influence a range of muscles crossing many joints. This divergence in the pathway from cortex to muscles has



been shown in several ways, including experiments that correlate the spiking of single cortical neurons with the activity of many arm muscles (Cheney and Fetz 1985) and experiments that correlate pulses of electrical current applied to a point in cortex with the activity of many arm muscles (Cheney et al. 1985; Park et al. 2001).

Similar complex, multijoint movements that resemble natural movements, evoked by stimulating motor cortex for 500 ms, have recently been observed in the cat and rat (Ethier et al. 2004; Haiss and Schwarz 2005). Rhythmic "chewing" movements have been obtained on long stimulation of the orofacial part of motor cortex in monkeys (Huang et al. 1989). Complex, multijoint movements with apparent behavioral significance have also been evoked by stimulation of specific regions of the posterior parietal lobe in monkeys and prosimians (Cooke et al. 2003; Stepienewska et al. 2005).

Single neurons tuned to direction or to complex, multijoint movement?

There is considerable debate over whether the activity of motor cortex neurons is better correlated with the Cartesian direction and speed of the hand during a reach or with the joint and muscle details of the reach (e.g., Georgopoulos et al. 1986; Graham et al. 2003; Holdefer and Miller 2002; Kakei et al. 1999; Moran and Schwartz 2000; Reina et al. 2001; Scott 2000; Todorov 2000). Neurons in motor cortex are undoubtedly direction tuned during reaching, but the directional tuning can change when the arm is placed in different initial positions or postures, leading to the suggestion that it is not hand movement per se but "intrinsic" or joint and muscle parameters that best correlate with the activity of the neurons (e.g., Caminiti et al. 1990; Graham et al. 2003; Scott and Kalaska 1995, 1997; Sergio and Kalaska 2003). In this view, the tuning for the direction of the hand in space is a consequence of a much more specific response function that might involve multiple joints or muscles.

The highly complex, multijoint, and sometimes multilimb movements that we obtained on stimulation have not been systematically studied in the single neuron literature. One possibility is that single neurons in motor cortex are tuned to these highly complex, multijoint movements that are frequently used by the monkey. Another possibility is that each neuron is tuned to a simpler movement and that the electrical stimulation activates pools of neurons to results in a complex movement. It will be useful to record the activity of motor cortex neurons during simpler movements such as directional reaching and during more complex movements such as hand-to-mouth movements, flinching movements, and manipulation movements. Will the activity of single neurons during these movements predict the effects of electrical stimulation of the same site in cortex?

Are the stimulation-evoked movements open-loop or closed-loop?

One hypothesis is that the cortical stimulation results in a fixed signal arriving at a set of muscles in an open-loop fashion. Several lines of evidence, however, suggest that the stimulation-evoked movements may represent a more complex adjustment or refinement of the movement by means of feedback rather than an open-loop pattern of output to the muscles.

In this study, we tested sites by attaching a lead weight to the wrist. Because the weight was concentrated at the wrist, it was predicted to have a large effect on the movement of the arm. The weight did significantly reduce the acceleration of the movement. However, for some cortical sites (74%), stimulation ultimately drove the hand to a similar final height as without the weight. In addition, for 94% of the sites, stimulation lifted the weighted hand to a greater height than was estimated for the case of no compensation. These findings suggest that, for at least some sites, the motor output may have been adjusted in a manner that compensated for the presence of the load. Not all sites, however, showed this compensation.

We also found that for some sites (54%), during stimulation, compensatory interactions between the joints helped to stabilize the hand and to bring it into a restricted range of positions. This result also suggests some possible refinement of the movement on the basis of feedback, in which the joint angles are adjusted to bring the hand to the correct location. It is worth noting, however, that the complex musculature of the arm makes it difficult to fully interpret this result. Is this effect the result of high-level coordination or the result of some unanticipated low-level muscle and torque interactions? One aspect of the result may be relevant to this question. We found the effect to be highly significant for some stimulation sites and found it to be absent for other stimulation sites, even though similar postures were evoked in both cases. This differing effect for different cortical sites suggests that the stabilization of the hand by means of joint interactions may have been a consequence of neuronal factors caused by stimulation of particular cortical sites and not a necessary consequence of the musculature of the arm. However, other interpretations of this result may be possible.

Perhaps the strongest evidence that feedback from the limb modifies the stimulation-evoked movement is that, when the arm is fixed in different positions, the stimulation evokes activity in different muscles. For example, consider a cortical site for which the final stimulation-evoked posture involves the elbow bent at a 90° angle. We found that when the elbow was fixed in an extended angle, stimulation evoked an initial increase in biceps EMG at about 7 ms latency, but little or no triceps activity (Graziano et al. 2004). When the elbow was fixed in a flexed angle, stimulation evoked an initial increase in triceps EMG at about 7 ms latency, but little or no biceps

FIG. 10. Topographic arrangement of stimulation effects. Rectangle on schematic brain shows approximate location of studied cortex. *A1*: clustering of different categories of movement in monkey 1. Diagonal line in map indicates lip of central sulcus, and area to left of line indicates unfolded cortex in anterior bank of sulcus. Curved line indicates location of arcuate sulcus as visualized during surgery. Sites are color-coded according to type of complex movement evoked. *A2*: similar map for monkey 2. Fewer sites were tested in monkey 2. *B1*: sites in monkey 1 were categorized according to whether the hand moved to a location within a 10-cm radius of a central point just in front of the chest (central point 12 cm vertically below chin) or moved outside of that central region of space. Dotted line indicates approximate border between arm representation (below line) and a combined leg and arm representation (above line). Fewer sites are shown here than in *A* because some of the sites in *A*, such as many of the sites related to defensive movements, did not involve clear movements of the contralateral arm. *B2*: similar map for monkey 2. *C1*: sites in monkey 1 were categorized according to whether the hand moved to upper space, middle space, or lower space. *C2*: similar map for monkey 2. *D1*: sites in monkey 1 were categorized according to whether the hand moved into space contralateral to the electrode, into middle space, or into ipsilateral space but showed no clear organization. *D2*: similar map for monkey 2.

activity. This pattern of activity was not consistent with the stimulation producing a fixed, open-loop signal arriving at the muscles.

Based on the lines of evidence described above, we propose that the movements evoked by electrical stimulation may represent a relatively high level of motor output. They combine many joints and body parts and are also to some degree adaptable depending on feedback, involving different muscle activity patterns and different final joint angles in different circumstances, possibly to achieve particular goal states. The results, however, are mixed; some sites show evidence of high-level, goal-directed motor control and other sites do not. For those sites that do show evidence of goal-directed motor control, it is not clear if the control mechanisms are spinal, cortical, or both.

Specialized subregions in the precentral gyrus

A set of studies suggested that a specialized region within the precentral gyrus may play a specific role in monitoring objects near the body and coordinating defensive reactions. These experiments showed that electrical stimulation of this zone evoked movements that matched in detail the normal defensive movements of a monkey (Cooke and Graziano 2003, 2004a). Neuronal activity in this region was correlated with the magnitude of a defensive reaction (Cooke and Graziano 2004a). Reversible activation and inactivation of this "defensive-like" cortical zone resulted in an up-regulation or down-regulation of the monkey's actual defensive movements to air puff (Cooke and Graziano 2004b). Thus it appears that this cortical zone may emphasize a particular ethological function. We hypothesize that other nearby cortical zones may emphasize other ethologically relevant movements, including hand-to-mouth movements; movements resembling a reach to distal space with the hand shaped as if to grasp; movements of the hand into central space in front of the chest accompanied by movement of the wrist and fingers into a pose that resembles manipulation of an object; and movements of all four limbs that we speculate may be related to locomotion. In this speculation, primary and premotor cortex may be composed of a mosaic of different cortical zones that emphasize different ethological functions.

Motor cortex topography may be determined by multiple competing factors

The topographic organization of motor cortex has been described in numerous previous studies (e.g., Donoghue et al. 1992; Foerster 1936; Fritsch and Hitzig 1870; Fulton 1938; Gould et al. 1986; Kwan et al. 1978; Park et al. 2001; Penfield and Boldrey 1937; Strick and Preston 1978; Woolsey et al. 1952). Most descriptions include a rough somatotopic organization with overlap between the representations of different body parts, some fractures in the representations, and some rerepresentations. These descriptions suggest that there may be other variables influencing the organization of motor cortex in addition to somatotopy.

The stimulation-evoked movements in this study were arranged in a complicated cortical topography shown in Fig. 10. No single movement parameter captured this topography. Instead, the organization seemed to be influenced by at least three different principles.

One type of organization obtained in this stimulation experiment was somatotopic, in which the face was represented more laterally and the legs were represented more medially, as expected on the basis of previous work. The somatotopy was not absolute. Leg, arm, and face representations were often intermingled.

A second organizational principle was the clustering of movements into cortical zones that, we hypothesize, may emphasize different ethological functions.

In a third type of organization, the evoked movements were arranged according to the location in space to which the hand moved. Hand locations near the chest were almost always evoked from a distinct posterior region of cortex that extended partly into the central sulcus. More distal hand locations, in which the hand projected away from the body, were typically evoked from more anterior regions of cortex. In addition, a map of hand elevation was found along the central sulcus, in which upper hand locations were more likely to be represented laterally and lower hand locations were more likely to be represented medially. This rough mapping of hand location across the cortical surface matched our previous findings (Graziano et al. 2002a).

In this study, the lateral position of the hand was not clearly mapped across the cortical surface. This finding is not consistent with our previous study (Graziano et al. 2002a), in which we found a clear topography of the lateral position of the hand in two monkeys. One possibility is that, in this experiment, the map was not explored extensively enough to reveal this dimension of the organization. Another possibility is that the topographic arrangement by hand position is simply variable from animal to animal.

The three types of organization, 1) by somatotopy, 2) by ethological function, and 3) by the spatial location of the hand, are not fully compatible with each other. It would be impossible to construct a map that perfectly preserves all three types of organization. We speculate that these three influences may compete for the topography in motor cortex, resulting in a fractured and somewhat multiply organized region of cortex. Somatotopic organization clearly dominates the large scale, in which the face is represented mainly laterally and the legs are represented mainly medially. Ethological function may influence the smaller scale, in which different ethologically relevant movement categories are clustered in different cortical zones. The location of the hand in space appears to be the weakest of the three influences, providing a partial and statistical topography of hand location.

ACKNOWLEDGMENTS

We thank T. Mole and S. Mixalot.

GRANTS

This study was supported by National Institutes of Health Grants EY-11347 and NS-046407 and Burroughs Wellcome Grant 992817.

REFERENCES

- Asanuma H and Arnold AP.** Noxious effects of excessive currents used for intracortical microstimulation. *Brain Res* 96: 103–107, 1975.
- Bizzzi E and Mussa-Ivaldi FA.** *Motor Control. Handbook of Neuropsychology*, edited by Boller F and Grafman J. New York: Elsevier, 1989, vol. 2, p. 229–244.
- Bruce CJ, Goldberg ME, Bushnell MC, and Stanton GB.** Primate frontal eye fields. II. Physiological and anatomical correlates of electrically evoked eye movements. *J Neurophysiol* 54: 714–734, 1985.

- Caminiti R, Johnson PB, and Urbano A. Making arm movements within different parts of space: dynamic aspects in the primate motor cortex. *J Neurosci* 10: 2039–2058, 1990.
- Cheney PD and Fetz EE. Comparable patterns of muscle facilitation evoked by individual corticomotoneuronal (CM) cells and by single intracortical microstimuli in primates: evidence for functional groups of CM cells. *J Neurophysiol* 53: 786–804, 1985.
- Cheney PD, Fetz EE, and Palmer SS. Patterns of facilitation and suppression of antagonist forelimb muscles from motor cortex sites in the awake monkey. *J Neurophysiol* 53: 805–820, 1985.
- Cooke DF and Graziano MSA. Defensive movements evoked by air puff in monkeys. *J Neurophysiol* 90: 3317–3329, 2003.
- Cooke DF and Graziano MSA. Sensorimotor integration in the precentral gyrus: polysensory neurons and defensive movements. *J Neurophysiol* 91: 1648–1660, 2004a.
- Cooke DF and Graziano MSA. Super-flinchers and nerves of steel: defensive movements altered by chemical manipulation of a cortical motor area. *Neuron* 43: 585–593, 2004b.
- Cooke DF, Taylor CSR, Moore T, and Graziano MSA. Complex movements evoked by microstimulation of the ventral intraparietal area. *Proc Natl Acad Sci USA* 100: 6163–6168, 2003.
- Denavit J and Hartenberg RS. A kinematic notation for lower-pair mechanisms on matrices. *J Appl Mech* 22: 215–221, 1955.
- Donoghue JP, LeBovic S, and Sanes JN. Organization of the forelimb area in squirrel monkey motor cortex: representation of digit, wrist, and elbow muscles. *Exp Brain Res* 89: 1–19, 1992.
- Ethier C, Imbeault M, Ung VR, and Capaday C. Vectorial addition of motor cortical outputs in the cat. *Soc Neurosci Abstr* 30: 872.14, 2004.
- Flash T and Hogan N. The coordination of arm movements: an experimentally confirmed experimental model. *J Neurosci* 5: 1688–1703, 1985.
- Foerster O. The motor cortex of man in the light of Hughlings Jackson's doctrines. *Brain* 59: 135–159, 1936.
- Freedman EG, Stanford TR, and Sparks DL. Combined eye-head gaze shifts produced by electrical stimulation of the superior colliculus in rhesus monkeys. *J Neurophysiol* 76: 927–952, 1996.
- Fritsch G and Hitzig E. Ueber die elektrische Erregbarkeit des Grosshirns. In: *The Cerebral Cortex*, edited by Nowinski WW, (Springfield, IL: Thomas, 1960), p. 73–96, 1870.
- Fulton JF. *Physiology of the Nervous System*. New York: Oxford, 1938, p. 399–457.
- Georgopoulos AP, Schwartz AB, and Kettner RE. Neuronal population coding of movement direction. *Science* 233: 1416–1419, 1986.
- Gottlieb JP, Bruce CJ, and MacAvoy MG. Smooth eye movements elicited by microstimulation in the primate frontal eye field. *J Neurophysiol* 69: 786–799, 1993.
- Gould HJ, Cusick CG, Pons TP, and Kaas JH. The relationship of corpus callosum connections to electrical stimulation maps of motor, supplementary motor, and the frontal eye fields in owl monkeys. *J Comp Neurol* 247: 297–325, 1986.
- Graham KM, Moore KD, Cabel DW, Gribble PL, Cisek P, and Scott SH. Kinematics and kinetics of multi-joint reaching in nonhuman primates. *J Neurophysiol* 89: 2667–2677, 2003.
- Graziano MSA, Cooke DF, Taylor CSR, and Moore T. Distribution of hand location in monkeys during spontaneous behavior. *Exp Brain Res* 155: 30–36, 2003.
- Graziano MSA, Patel KT, and Taylor CSR. Mapping from motor cortex to biceps and triceps altered by elbow angle. *J Neurophysiol* 92: 395–407, 2004.
- Graziano MSA, Taylor CSR, and Moore T. Complex movements evoked by microstimulation of precentral cortex. *Neuron* 34: 841–851, 2002a.
- Graziano MSA, Taylor CSR, Moore T, and Cooke DF. The cortical control of movement revisited. *Neuron* 36: 349–362, 2002b.
- Haiss F and Schwarz C. Spatial segregation of different modes of movement control in the whisker representation of rat primary motor cortex. *J Neurosci* 25: 1579–1587, 2005.
- Holdefer RN and Miller LE. Primary motor cortical neurons encode functional muscle synergies. *Exp Brain Res* 146: 233–243, 2002.
- Huang CS, Hiraba H, Murray GM, and Sessle BJ. Topographical distribution and functional properties of cortically induced rhythmical jaw movements in the monkey (*Macaca fascicularis*). *J Neurophysiol* 61: 635–650, 1989.
- Kakei S, Hoffman D, and Strick P. Muscle and movement representations in the primary motor cortex. *Science* 285: 2136–2139, 1999.
- Kwan HC, MacKay WA, Murphy JT, and Wong YC. Spatial organization of precentral cortex in awake primates. II. Motor outputs. *J Neurophysiol* 41: 1120–1131, 1978.
- Lu X and Ashe J. Anticipatory activity in primary motor cortex codes memorized movement sequences. *Neuron* 45: 967–973, 2005.
- Luh JYS, Walker MW, and Paul RPC. On-line computational scheme for mechanical manipulators. *J Dynamic Syst Measure Control* 102: 69–76, 1980.
- Moran DW and Schwartz AB. One motor cortex, two different views. *Nat Neurosci* 3: 963, 2000.
- Park MC, Belhaj-Saif A, Gordon M, and Cheney PD. Consistent features in the forelimb representation of primary motor cortex in rhesus macaques. *J Neurosci* 21: 2784–2792, 2001.
- Penfield W and Boldrey E. Somatic motor and sensory representation in the cerebral cortex of man as studied by electrical stimulation. *Brain* 60: 389–443, 1937.
- Reina GA, Moran DW, and Schwartz AB. On the relationship between joint angular velocity and motor cortical discharge during reaching. *J Neurophysiol* 85: 2576–2589, 2001.
- Robinson DA and Fuchs AF. Eye movements evoked by stimulation of the frontal eye fields. *J Neurophysiol* 32: 637–648, 1969.
- Romo R, Hernandez A, Zainos A, and Salinas E. Somatosensory discrimination based on cortical microstimulation. *Nature* 392: 387–390, 1998.
- Salzman CD, Britten KH, and Newsome WT. Cortical microstimulation influences perceptual judgements of motion direction. *Nature* 346: 174–177, 1990.
- Scott SH. Reply to one motor cortex, two different views. *Nat Neurosci* 3: 964–965, 2000.
- Scott SH and Kalaska JF. Changes in motor cortex activity during reaching movements with similar hand paths but different arm postures. *J Neurophysiol* 73: 2563–2567, 1995.
- Scott SH and Kalaska JF. Reaching movements with similar hand paths but different arm orientations. I. Activity of individual cells in motor cortex. *J Neurophysiol* 77: 826–852, 1997.
- Sergio LE and Kalaska JF. Systematic changes in motor cortex cell activity with arm posture during directional isometric force generation. *J Neurophysiol* 89: 212–228, 2003.
- Stepniewska I, Fang PC, and Kaas JH. Microstimulation reveals specialized subregions for different complex movements in posterior parietal cortex of prosimian galagos. *Proc Natl Acad Sci USA* 102: 4878–4883, 2005.
- Strick PL and Preston JB. Multiple representation in the primate motor cortex. *Brain Res* 154: 366–370, 1978.
- Tehovnik EJ. Electrical stimulation of neural tissue to evoke behavioral responses. *J Neurosci Methods* 65: 1–17, 1996.
- Tehovnik EJ and Lee K. The dorsomedial frontal cortex of the rhesus monkey: topographic representation of saccades evoked by electrical stimulation. *Exp Brain Res* 96: 430–442, 1993.
- Todorov E. Direct cortical control of muscle activation in voluntary arm movements: a model. *Nat Neurosci* 3: 391–398, 2000.
- Walker MW and Orin DE. Efficient dynamic computer simulation of robotic mechanisms. *J Dynamic Syst Measure Control* 104: 205–211, 1982.
- Woolsey CN, Settlage PH, Meyer DR, Sencer W, Hamuy TP, and Travis AM. Pattern of localization in precentral and “supplementary” motor areas and their relation to the concept of a premotor area. In: *Association for Research in Nervous and Mental Disease*. New York: Raven Press, 1952, vol. 30, p. 238–264.